

# A Method for Transient Torque Response Improvement in Optimum Efficiency Induction Motor Drives

Slobodan N. Vukosavic, *Member, IEEE*, and Emil Levi, *Senior Member, IEEE*

**Abstract**—Optimal efficiency control of induction motor drives implies operation at reduced flux levels with light loads. Two problems in light load operation are a large speed drop after sudden load torque increase and slow acceleration. In order to improve response in these transients, an algorithm for optimum dynamic distribution of the available maximum inverter current into the flux-producing and the torque-producing stator current components is developed in this paper. The proposed algorithm accounts for the main flux saturation effect in the machine and the dynamics of the flux variation. Its performance is illustrated by means of simulation and experimental results. Superiority of the developed algorithm over some of the existing methods is proved by comparing the speed drops, which result after sudden load torque increase during operation at light load, and by examining an acceleration transient under light load condition.

**Index Terms**—Current limit, disturbance rejection, induction motor drives, main flux saturation, vector control.

## I. INTRODUCTION

THE torque delivered by induction motor drives (IMDs) comes as a product of two adjustable variables, namely, the flux amplitude and the active component of the stator current. Existing degree of freedom provides the means for reducing the power conversion losses or attaining other performance criteria through the flux level adjustment. Since the onset of the IMD frequency control, efforts were made to improve the IMD efficiency by varying the flux amplitude for a better balance between core and copper losses. The IMD power loss reduction is achieved by implementing a loss minimization controller. The benefit of this approach is its applicability to standard, off-the-shelf induction motors. Worthy results have been achieved over the last two decades, as summarized in a number of excellent surveys [1]–[3]. In [2], an extensive overview with over 100 references identifies three distinct approaches to optimum efficiency (minimum loss) control: i) a simple state controller; ii) a loss model-based controller; and iii) a search controller.

Regardless of which type of the loss minimization controller is applied, an induction motor will always be operated with reduced flux level at light loads. The problems that arise at light load operation are how to achieve the minimum time response

(i.e., a minimum speed drop) if a sudden load change takes place and how to minimize the duration of an acceleration transient after step speed command increase. The maximum available stator current is always limited by the inverter rating. Therefore, the problem reduces to the determination of the optimal subdivision of the available maximum current into the flux-producing and torque-producing stator current components, so that the maximum dynamic torque is developed while simultaneously re-establishing the rated flux in the motor. Optimum efficiency control is normally disabled during such transients and the current subdivision is performed according to a certain algorithm. The simplest solution, that preserves full decoupling between the flux and torque production, is to retain the existing value of the flux producing current and use all of the available inverter current capability to increase the torque producing current [4]. This method is, however, characterized with very slow transient response and is therefore not considered as a viable solution. Another possibility, proposed in [5], is to reset the flux-producing stator current component to the rated value once when the transient is detected. The remaining current capability of the inverter is then used for the torque producing current component. This method is simple to implement and is widely used in the existing literature [6]–[9].

An alternative method for the maximum current subdivision into the transient flux-producing and torque-producing stator current components is the one of [10] and [11]. The method is developed by considering dynamics of the vector controlled induction motor drive and by recognizing the importance of accounting for the main flux saturation in the given solution to the problem. It is recommended to apply at first all of the available current to the flux-producing current component, so that dynamic torque is initially zero. Once when the forced flux build-up is completed, all of the available inverter current is switched into the torque-producing current component. Substantial torque is developed, since the trapped rotor flux is utilized for this purpose. As shown in [10] and [11], utilization of this strategy enables development of much higher transient torque than the simpler method of resetting the flux-producing current component to the rated value.

The shortest duration of the transient results if some kind of flux forcing is applied during the transition from the low to the high flux level. Any method of maximum current subdivision into optimal flux- and torque-producing current components has therefore to account for the main flux saturation in the machine, as observed in [10], [11]. In this context, some other attempts to improve the torque response during a transient [12], [13], by

Manuscript received December 19, 2001; revised July 3, 2002.

S. N. Vukosavic is with the University of Belgrade, Electrical Engineering Faculty, Belgrade 11000, Yugoslavia (e-mail: boban@ieee.org).

E. Levi is with the Liverpool John Moores University, School of Engineering, Liverpool L3 3AF, U.K. (e-mail: e.levi@livjm.ac.uk).

Digital Object Identifier 10.1109/TEC.2003.816599

essentially keeping the flux-and torque producing current components mutually equal (which is the condition of maximum steady-state torque development under unsaturated conditions) are of limited value in practice.

None of the techniques described so far attempts to achieve minimization of the speed drop after a sudden load torque increase or minimization of the acceleration transient duration after sudden increase in the speed command. Another type of solution, available in the literature, consists of continuous variation of the two current components during operation in the current limit, according to a predefined law. For example, it is proposed in [14] to vary the torque producing current as a predefined linear function of the flux and to use the remainder of the available inverter current for the flux producing current. The flux producing current is reset to the rated value once when the torque-producing current reaches 95% of its limit. The predefined law used in [14] is of ad-hoc nature and, although it does present an improvement over the simple resetting of the flux-producing current to the rated value, it does not minimize a speed drop or transient duration.

A more sophisticated and much more difficult to implement is the method described in [15]. It is developed using a very simplified representation of the machine's magnetizing curve (linear flux variation, followed by constant flux value in the saturated region), on the basis of the optimal control theory, and is examined by simulation only. The case studied is the start-up of the machine with zero initial conditions for flux and speed, with the requirement that the known set speed is reached in the minimum time with the given current limit. The important conclusions of [15] are that saturation of the motor has to be considered for any realistic optimal solution, and that the flux-producing and torque-producing stator current components have to continuously vary during the transient within the given current limit, in order to achieve the minimum response time. The method of [15] has however never been considered as a mean for minimizing the speed drop after a sudden load torque increase, which is a different problem compared to the start-up with known speed reference.

The problem of slow torque build-up at low flux levels is associated with the delay in the flux response to the applied (increased) flux-producing current component. A potential solution, considering the limited current capability of the inverter, is utilization of an additional P or PI controller within the control system of a rotor flux oriented induction machine [16]. The role of this additional controller is to provide forced magnetization during the transient, by forcing the flux-producing current to a value higher than rated. The remaining current capability of the inverter is then used for the torque-producing current. This approach however does not secure minimization of the speed drop during sudden load torque change and is therefore not considered further on.

This paper is concerned with the optimal dynamic stator current distribution into the flux-producing and the torque-producing current components in the base speed region, in the presence of the limited current capability of the inverter and sufficient inverter voltage reserve. An indirect rotor flux oriented induction motor drive is considered in conjunction with an optimal efficiency, loss model-based controller. A

novel algorithm for dynamic determination of the optimal stator  $d$ -axis and  $q$ -axis current commands is developed. The criterion used for the algorithm development is that the speed drop due to sudden load torque increase (or the speed error due to sudden speed command increase), which takes place from a steady state with light load, has to be of minimal value. Optimal efficiency control is switched off during the transient. Main flux saturation and dynamics of the rotor flux are fully accounted for in the algorithm. The proposed algorithm is verified by performing at first simulation and then experiments on two vector controlled induction motor drives. Its superior performance, when compared to some of the existing methods, is proved by comparing the speed drops that result after sudden load torque increase at low flux level (light load) condition and by examining an acceleration transient under light load condition. Some important implementation-related issues are addressed as well.

## II. ALGORITHM FOR OPTIMUM TRANSIENT CURRENT DISTRIBUTION

### A. Statement of the Problem

Let an indirect rotor flux oriented induction machine operate in steady state at light load, with reduced rotor flux level and with optimum efficiency. In such a steady state, assuming ideal rotor flux oriented control, one has

$$\begin{aligned} i_{ds1}^* &= i_{ds1} & i_{qs1}^* &= i_{qs1} \\ \psi_{r1}^* &= \psi_{r1} = L_m i_{ds1} & \omega_{sl1}^* &= \frac{L_m R_r}{L_r} \frac{i_{qs1}^*}{\psi_{r1}^*} \\ T_{e1}^* &= T_{e1} = T_{L1} & T_{e1}^* &= \left(\frac{3}{2}\right) P \left(\frac{L_m}{L_r}\right) \psi_{r1}^* i_{qs1}^* \end{aligned} \quad (1)$$

Here asterisk denotes commanded (reference) values, indices  $d$  and  $q$  identify  $d$ - $q$  axis components of the stator current  $i_s$ ,  $\psi_r$  is the rotor flux,  $\omega_{sl}$  and  $T_e$  stand for rotor angular slip frequency and motor torque, respectively,  $P$  is the number of pole pairs,  $T_L$  is the load torque,  $R_r$  is the rotor resistance, and  $L_m$  and  $L_r$  are the magnetizing inductance and rotor self-inductance, respectively. A sudden step load torque increase takes place next, at time instant zero, leading to the operation of the inverter at maximum allowed current value  $i_{s\max}$ . The available current is to be distributed somehow into the  $d$ - and  $q$ -axis current commands, so that during the transient

$$i_{s\max} = \sqrt{i_{ds}^{*2} + i_{qs}^{*2}} \quad (2)$$

where  $i_{s\max}$  is the maximum allowed value of the stator current. The two existing methods, which will be later on compared with the algorithm that is to be developed here, are characterized with the following maximum available current distribution.

- i) Resetting the  $d$ -axis current to the rated value (index  $n$ )

$$i_{ds}^* = i_{dsn} \quad i_{qs}^* = \sqrt{i_{s\max}^2 - i_{dsn}^2} \quad (3)$$

- ii) Applying all of the current initially to the  $d$ -axis, with subsequent switching into  $q$ -axis

$$\begin{aligned} i_{ds}^* &= i_{s\max} & i_{qs}^* &= 0 & \text{for } 0 < t < t_1 \\ i_{ds}^* &= 0 & i_{qs}^* &= i_{s\max} & \text{for } t_1 < t < t_2. \end{aligned} \quad (4)$$

Upon resetting the  $d$ -axis current to the rated value, the rotor flux (and hence, the torque generating capability) variation is characterized by the rotor time constant  $T_r$ , according to

$$\psi_r + T_r \frac{d\psi_r}{dt} = L_m i_{ds} \quad (5)$$

and is therefore inherently slow. Initial assignment of the full maximum current to the  $d$ -axis (as in the second method) causes forced rotor flux build-up, at the expense of zero torque production during the first interval. Thus, neither of the two approaches provides minimization of the speed drop (or the speed error)  $\Delta\omega_{\max}$  during the transient. A dynamic current sharing strategy is therefore developed, respecting the saturation phenomenon, conceived to result in a minimum possible speed drop, that is defined with

$$\Delta\omega_{\max} = \frac{1}{J} \int_0^{t_x} (T_L - T_e(t)) dt$$

$$T_e(t_x) = T_L. \quad (6)$$

Here  $J$  is the total inertia of the drive. The problem thus reduces to finding the optimal trajectories

$$\begin{aligned} i_{ds}^* &= i_{ds}^*(t) \\ i_{qs}^* &= i_{qs}^*(t) \end{aligned} \quad (7)$$

subject to initial conditions and the constraint

$$\begin{aligned} i_{ds}^*(0) &= i_{ds1}, \quad i_{qs}^*(0) = i_{qs1} \\ i_{ds}^{*2}(t) + i_{qs}^{*2}(t) &= i_{s\max}^2 \end{aligned} \quad (8)$$

so that the speed drop  $\Delta\omega_{\max}$  of (6) is minimized.

Direct and exact minimization of (6) requires knowledge of the instant  $t_x$  when the speed drop attains maximum value. This instant is not known in advance and (6) will therefore have to be reformulated, as discussed shortly. Next, utilization of (6) requires that the load torque value is known. The strategy of the optimum current sharing, that is to be developed further in this section, is ideally suited to those drives where the load torque impact is predictable and the value of the load torque in (6) can therefore be set appropriately. However, developed strategy is useful even when the load torque value is not known. In such cases, load torque in (6) should be set to the maximum anticipated value for a given drive. Improvement in the speed drop reduction will be smaller than when the load torque value is known in advance, but will nevertheless exist, as shown by experimental investigation in Section III.

### B. Saturation Related Issues

Rotor flux variation during a transient, given with (5), is valid only under the assumption of the linear magnetic circuit. Such an assumption is here not admissible since forced rotor flux build-up is required. It is therefore necessary to modify (5), so that it accounts for the main flux saturation. Inverse magnetizing curve of the machine  $i_m = f(\psi_m)$  is assumed to be known ( $i_m$  and  $\psi_m$  denote magnetizing current and magnetizing flux space

vector magnitudes, respectively). It can be represented with a simple analytical function [17]:

$$\left( \frac{i_m}{i_{mn}} \right) = \beta \left( \frac{\psi_m}{\psi_{mn}} \right) + (1 - \beta) \left( \frac{\psi_m}{\psi_{mn}} \right)^S. \quad (9)$$

Index  $n$  in (9) stands for rated (nominal) values of the magnetizing flux and the magnetizing current (index  $m$ ), and parameters of the function ( $\beta$  and  $S$ ) are machine specific. For standard induction motors, parameters  $\beta = 0.7$  and  $S = 9$  provide precise estimation of the magnetizing current up to flux levels of 1.1 (p.u.) [17]. In the case of high efficiency motors [15], the saturation is less emphasized due to a lower flux density, and the best fit for the parameter  $\beta$  in (9) shifts toward  $\beta = 0.9$  [17]. The function (9) becomes inaccurate as the flux level reduces below 0.1 (p.u.), where the magnetizing curve bands and inflects as it comes closer to the origin. However, for the flux range of practical interest (which is always at least 10% and extends to no more than 110%), the approximation (9) with  $\beta = 0.7$  and  $S = 9$  is sufficiently accurate for practical implementation in conjunction with standard induction motors. In such a way, parameter setting is limited to the definition of the rated values ( $i_{mn}$ ,  $\psi_{mn}$ ) on the magnetizing curve, that have to be known anyway in any implementation of the rotor flux oriented control.

In a rotor flux oriented induction machine, contribution of the  $q$ -axis magnetizing flux to the overall magnetizing flux is negligibly small for all of the practically realizable torque values (up to three times the rated motor torque) in transient operation, so that the cross saturation effect can be neglected [18]. It is therefore permissible to equate in (9) the  $d$ -axis magnetizing flux with the total magnetizing flux and the  $d$ -axis magnetizing current with the total magnetizing current

$$i_{dm} \approx i_m, \quad \psi_{dm} \approx \psi_m. \quad (10)$$

This enables an alternative formulation of the rotor flux dynamic (5), using defining rotor flux equation in the rotor flux oriented reference frame ( $R_r i_{dr} + d\psi_r/dt = 0$ ) as the starting point, as

$$\frac{d\psi_r}{dt} = R_r (i_{ds}^* - i_{dm}(\psi_{dm})) \quad (11)$$

since under ideal field orientation  $i_{ds}^* = i_{ds}$ , and rotor current  $d$ -axis component is  $i_{dr} = i_{dm} - i_{ds}$ . Equation (11) fully accounts for the saturation of the magnetizing flux, since the function  $i_{dm}(\psi_{dm})$  represents, according to (10), inverse magnetizing curve approximation of (9). Correlation between  $d$ -axis magnetizing flux and rotor flux is given with

$$\psi_{dm} = \psi_r + L_{\sigma r} (i_{ds}^* - i_{dm}) \quad (12)$$

where  $L_{\sigma r}$  is the rotor leakage inductance.

Nonlinear rotor flux estimator, described with (11) and (12), is schematically shown in Fig. 1, together with the remainder of the indirect rotor flux oriented controller. The inputs in Fig. 1 (stator  $d$ -axis current reference and torque) are in steady state operation provided by the optimal efficiency controller and the speed controller, respectively. During transients, stator  $d$ -axis and  $q$ -axis current references are obtained using optimum dynamic current sharing technique, that is explained in the next

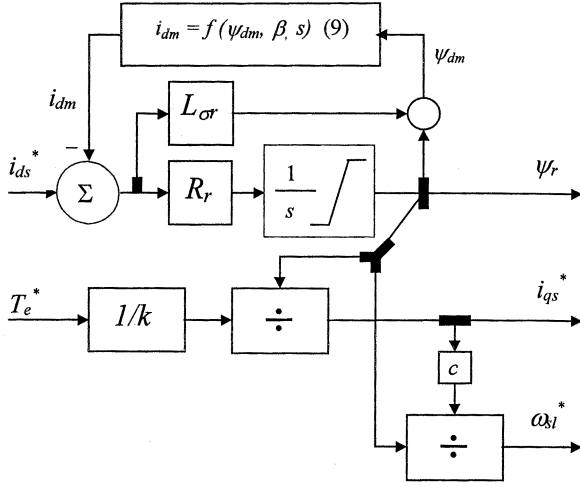


Fig. 1. Nonlinear rotor flux estimator and the indirect vector controller with compensation of main flux saturation.

subsection. Calculation of the reference angular speed and the nonlinear rotor flux estimator in Fig. 1 remain active during the transient as well. The ratio  $L_m/L_r$  in the torque and angular slip frequency equations of (1) changes insignificantly with the change in the saturation level and can therefore be regarded as constant and equal to the one for the rated operating point at the magnetizing curve [19]. The constants  $k$  and  $c$  in Fig. 1 therefore stand for  $k = (3/2)P(L_{mn}/L_{rn})$  and  $c = R_r L_{mn}/L_{rn}$ .

### C. Algorithm for Optimum Current Distribution Following Sudden Load Torque Change

As already noted, (6) cannot be solved directly since the instant when motor torque becomes equal to the load torque is not known. However, in order to provide the minimum speed drop in (6), rotor flux has to monotonically increase during the transient. With this in mind, it is proposed to reformulate (6) and express the speed drop as function of the rotor flux change, rather than time. The time increment  $dt$  can be written from (11) as

$$dt = \frac{d\psi_r}{[R_r(i_{ds}^* - i_{dm}(\psi_{dm}))]} \quad (13)$$

Substitution into (6) and change of the borders of integration yields

$$\Delta\omega_{\max} = \frac{1}{J} \int_{\psi_r(0)}^{\psi_r(t_x)} \frac{T_L - k\psi_r i_{qs}^*}{R_r(i_{ds}^* - i_{dm}(\psi_{dm}))} d\psi_r. \quad (14)$$

Note that, for any given stator  $d$ -axis current command, rotor flux and  $d$ -axis magnetizing current component in (14) are determined with (9)–(12) (i.e., with the nonlinear flux estimator in Fig. 1). Next, it is assumed that during the transient, stator current is in the limit. Hence, reference stator  $d$ - $q$  axis currents can be written as

$$i_{ds}^* = i_{s\max} \cos \theta(t), \quad i_{qs}^* = i_{s\max} \sin \theta(t) \quad (15)$$

or, using an alternative formulation in terms of rotor flux variation

$$i_{ds}^* = i_{s\max} \cos \theta(\psi_r), \quad i_{qs}^* = i_{s\max} \sin \theta(\psi_r). \quad (16)$$

Here, angle  $\theta$  denotes instantaneous position of the stator current reference space vector with respect to the  $d$ -axis of the reference frame. Substitution of (16) into (14) leads to the final form of the maximum speed drop that is to be minimized online by means of the optimal current subdivision

$$\Delta\omega_{\max} = \frac{1}{JR_r} \int_{\psi_r(0)}^{\psi_r(t_x)} \frac{T_L - k\psi_r i_{s\max} \sin \theta(\psi_r)}{i_{s\max} \cos \theta(\psi_r) - i_{dm}(\psi_{dm})} d\psi_r. \quad (17)$$

The problem of optimal current distribution therefore reduces to determination of the optimal  $\theta(\psi_r)$  values within the interval  $[\psi_r(0) \dots \psi_r(t_x)]$ .

Integration in (17) reduces to summation in a real time application, since discrete time instants are under consideration. Contribution of each individual sample to the overall maximum speed drop will be minimized if and only if, for each discrete value of the rotor flux (i.e., in each discrete time instant), the value of the angle  $\theta$  is such that the function under the integral is of the minimum possible value. This consideration is valid since the selection of the angle  $\theta$  for one particular value of the rotor flux has no impact whatsoever on the value of the integrand for other rotor flux values. In other words, the problem of finding the optimum angle  $\theta$  value for a given rotor flux value translates into finding the minimum of the integrand in (17) with respect to angle  $\theta$  in each sampling interval. Thus, the equation

$$\frac{d}{d\theta} \left( \frac{T_L - k\psi_r i_{s\max} \sin \theta(\psi_r)}{i_{s\max} \cos \theta(\psi_r) - i_{dm}(\psi_{dm})} \right) = 0 \quad (18)$$

provides the means for solving for the optimum  $\theta$  value for a given pair of rotor flux and  $d$ -axis magnetizing current values

$$k\psi_r i_{s\max} i_{dm}(\psi_{dm}) \cos \theta(\psi_r) + T_L i_{s\max} \sin \theta(\psi_r) = k\psi_r i_{s\max}^2. \quad (19)$$

Note that both the numerator and the denominator of (18) are positive during the time interval to which the analysis applies (0 to  $t_x$ ). Division of (19) with the term on the right-hand side, substitution  $x = \sin \theta$  and introduction of two variable coefficients

$$\alpha = \frac{i_{dm}(\psi_{dm})}{i_{s\max}}, \quad \beta = \frac{T_L}{(k\psi_r i_{s\max})} \quad (20)$$

reduces (19) to a quadratic equation

$$(\alpha^2 + \beta^2)x^2 - 2\beta x + (1 - \alpha^2) = 0. \quad (21)$$

The quadratic equation (21) is to be solved online in each sampling interval, since the coefficients (20) vary in time (because rotor flux and  $d$ -axis magnetizing current change continuously). The solution is

$$x = \sin \theta = 0.5(p - \sqrt{p^2 - 4q}) \quad (22)$$

where  $p = 2\beta/(\alpha^2 + \beta^2)$  and  $q = (1 - \alpha^2)/(\alpha^2 + \beta^2)$ . The coefficients are such that  $\alpha < 1$ ,  $p > 0$ ,  $q > 0$ , and  $0 < x < 1$ . From the two possible solutions of (21), the one with the negative sign applies, as indicated in (22) (this has been verified during the course of investigation; the proof is cumbersome and is therefore omitted). Once when  $\sin \theta$  is calculated using (22),  $\cos \theta$  can be found as  $\cos \theta = \sqrt{1 - \sin^2 \theta}$ . Stator  $d$ - and  $q$ -axis

current references are then determined with (16). Note that the value of the angle  $\theta$  itself is of no interest.

It is important to note that the developed procedure is active only in the time interval during which the speed is reducing. At the time instant  $t_x$ , when motor torque becomes equal to the load torque [i.e., the numerator of (17) becomes equal to zero], the speed starts to increase. At this point in time, the flux-producing current is reset to its rated value and torque-producing current is driven to the maximum value of  $i_{qs}^* = \sqrt{i_{s\max}^2 - i_{dsn}^2}$ .

#### D. Summary of the Procedure

Once when the load impact is detected, optimum efficiency control is disabled and the algorithm for optimum current distribution during the transient, described in the preceding section, is activated. On the basis of the known stator  $d$ -axis current reference in the previous sampling instant, an evaluation of the rotor flux and  $d$ -axis magnetizing current values is performed using the nonlinear flux estimator of Fig. 1 ((9), (11), (12), with (10) accounted for). Next, the load torque in (17) is set to either the known value or the maximum anticipated value for the given drive. Coefficients  $\alpha$  and  $\beta$  of (20) are calculated using the known maximum stator current of (2) and values of  $i_{dm}(\psi_{dm})$ ,  $\psi_r$ , and  $T_L$ . Required  $\sin\theta$  for optimal current sharing is then calculated from (22) and  $\cos\theta$  is found from  $\cos\theta = \sqrt{1 - \sin^2\theta}$ . Finally, stator  $d$ - $q$  axis current references for the next sampling interval are formed using (16). The procedure is repeated in each sampling interval.

#### E. Implementation Related Issues

The major difficulty in the implementation of the developed algorithm represents calculation of the square root function. This operation appears twice in the algorithm, at first in (22) ( $\sin\theta$  calculation) and then in evaluation of  $\cos\theta$ . In both cases, the number under the square root is smaller than one.

The implementation of the described algorithm was carried out using a TMS320F243 DSP, in which number 1 is represented in Q15 format as 7FFF. The procedure for finding the square root of a certain number "argument," whose value is between zero and one, is the following. The argument is multiplied by 4 (i.e., shifted to the left twice) as many times as it is necessary to bring the value into the interval 0.25 to 1 (i.e.,  $X_{\text{arg}}^{\text{in}} = \text{argument} \times 4^n$ ). The reason for this is that a small value of the "argument" would require a large number of iterations in the process of finding the square root value. An initial guess is set next, as  $Y_{\text{arg}}^{\text{new}} = X_{\text{arg}}^{\text{in}}$ . A recurrent formula

$$Y_{\text{arg}}^{\text{new}} = Y_{\text{arg}}^{\text{old}} - \frac{[(Y_{\text{arg}}^{\text{old}})^2 - X_{\text{arg}}^{\text{in}}]}{2} \quad (23)$$

is applied seven times. The result is finally found as

$$\sqrt{\text{argument}} = \frac{Y_{\text{arg}}^{\text{new}}}{2^n} \quad (24)$$

where number  $n$  is the one applied initially to move the argument into the 0.25–1 interval. This procedure enables implementation of the algorithm in real time.

### III. VERIFICATION OF THE PROPOSED ALGORITHM

#### A. Simulation Results

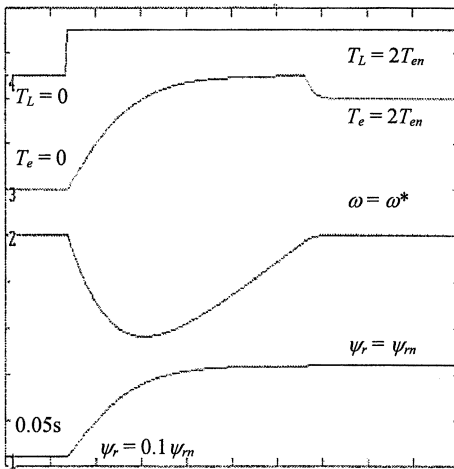
The proposed algorithm for minimization of the speed drop, described in the previous section, is at first tested using simulation. A 50-Hz, 1-kW, 380-V, 2.8-A four-pole induction machine is considered. The motor model used in the simulation fully accounts for the saturation effect (including dynamic cross-saturation effect, [18]). The motor initially operates in steady state under no-load conditions and with rotor flux equal to 10% of the rated rotor flux value. Load torque is then stepped to 200%, with this value being used in calculations related to (20)–(22). Inverter current is limited to twice the rated stator current of the motor. Performance of the algorithm developed here is shown in Fig. 2, along with the performance of the two existing algorithms described with (3) and (4).

As can be seen from Fig. 2, the proposed method of optimum dynamic current sharing of the limited inverter maximum current capability leads to by far the smallest drop in speed, when compared with the other two methods. Consequently, the time interval needed for the motor speed to return to the reference value is the shortest.

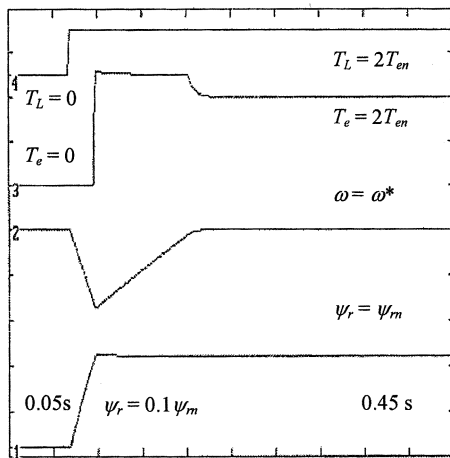
#### B. Experimental Verification

Experimental verification is performed using two different motors. The first one is the 1-kW motor already studied in simulation. The motor initially operates under no-load conditions at the steady state speed of 750 r/min, that is maintained by the speed controller. It is coupled to a dc machine, so that the motor torque is approximately 8% of the rated value, due to the combined losses of the two coupled machines. Rotor flux value is determined by the optimal efficiency controller and is 20% of the rated value in the no-load operation. The load torque is then stepped to 200% of the rated value [this value of load torque is used in (20)–(22)]. Inverter current is limited to twice the rated motor current. Fig. 3 illustrates experimentally recorded speed trace and the rotor flux variation (obtained from the output of the nonlinear flux estimator in Fig. 1) for the proposed strategy and for the basic strategy of resetting the  $d$ -axis current reference to the rated value. As can be seen from Fig. 3, speed drop is 98 r/min if the  $d$ -axis current is reset to the rated value. Speed restoration time is over 250 ms. In contrast to this, the strategy proposed here reduces the speed drop to 58 r/min, so that the speed restoration time is around 175 ms.

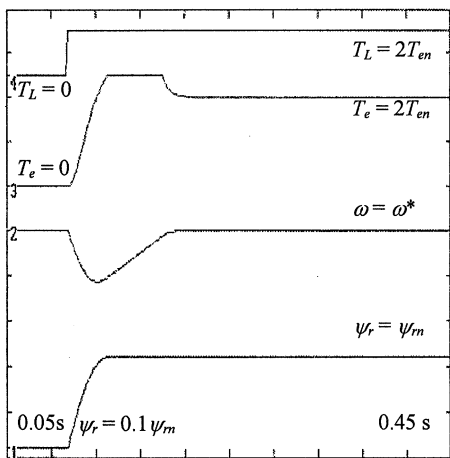
Further experimentation is performed next using a 2.2-kW, 50-Hz, four-pole induction motor. The motor under test is coupled to a separately excited dc machine with the armature winding connected to a variable noninductive resistor via a fast circuit breaker used for the load torque step change simulation. Torque, flux, and speed controllers are coded in assembler language on a 16-b digital signal processor (DSP) used within a standard industrial servo-amplifier *MOOG DBS 8/22*. The indirect rotor flux oriented controller structure comprises a digital current controller running at a 10-kHz sampling rate and the speed controller with  $T_{\text{sp1}} = 200 \mu\text{s}$ . Optimal current sharing routines are executed at a rate of 2 kHz (500  $\mu\text{s}$ ). The drive operates initially under no-load conditions (the motor torque is around 5% of the rated value, due to the combined



(a)



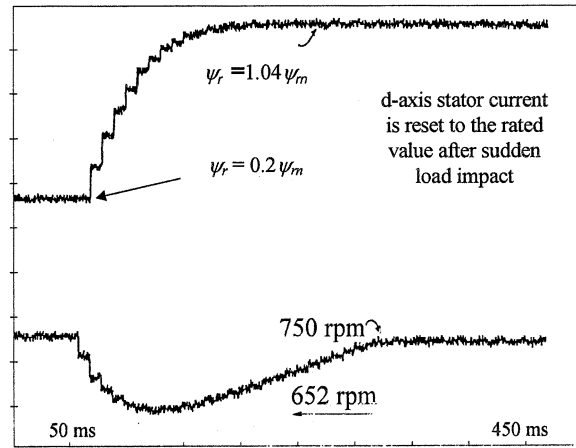
(b)



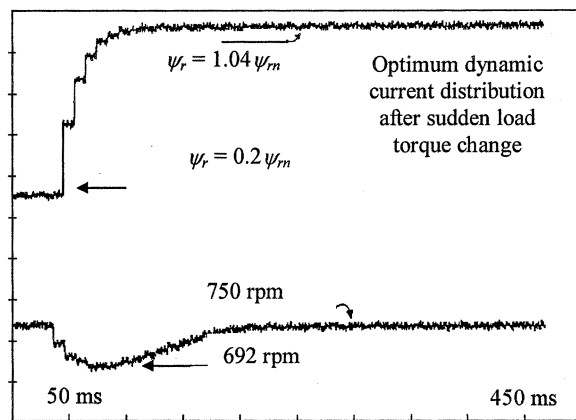
(c)

Fig. 2. Response of the drive to sudden load impact from light load condition with three methods of limited stator current distribution: (a) resetting of stator *d*-axis current to the rated value; (b) application of  $i_{s \max}$  to initially *d*-axis with subsequent switchover to *q*-axis; (c) proposed algorithm described in this paper.

losses of the two coupled machines), with rotor flux set by the optimum efficiency controller (approximately 20% of the rated value). Two cases are considered and for both of them, the load torque in (20) is set to the same value of 25 Nm (rated torque is 15 Nm). Stator current limit equals twice the rated motor



(a)



(b)

Fig. 3. Experimental results for the 1-kW motor, showing motor speed and rotor flux variation for (a) resetting of *d*-axis current to the rated value; (b) application of the algorithm proposed in this paper.

current and the operating speed of the motor is in both cases 157 rad/s.

Load torque is at first stepped to 25 Nm [i.e., the value used in (20)]. Fig. 4 shows variation of the stator *d*-axis current command, stator *q*-axis current command, and the total stator current during this transient when the optimal current sharing is applied. The same traces are shown in Fig. 5 for the case of resetting the stator *d*-axis current to the rated value, while a comparison of the resulting speed drop for the two methods is given in Fig. 6. All of the currents are given in per unit, using rated stator current as the base. Rated *d*-axis current of the machine on the rated stator current base is 0.7 p.u. In initial steady state with light load stator *d*-axis current is around 0.1 p.u., which corresponds, on the basis of the machine's magnetizing curve (9), to approximately 20% of the rated rotor flux.

As can be seen from Figs. 4 and 5, operation in the stator current limit of 2 p.u. takes place in both cases. In the case of stator *d*-axis current resetting to the rated value, stator *d*-axis current is 0.7 p.u. while the *q*-axis current is 1.87 p.u. and both stay at the constant value during the operation in the stator current limit. Contrary to this, the proposed algorithm with optimal dynamic current sharing causes an initial *d*-axis current increase to 1.95 p.u., that leads to the forced rotor flux build-up. Stator *q*-axis current however simultaneously starts increasing as well, while

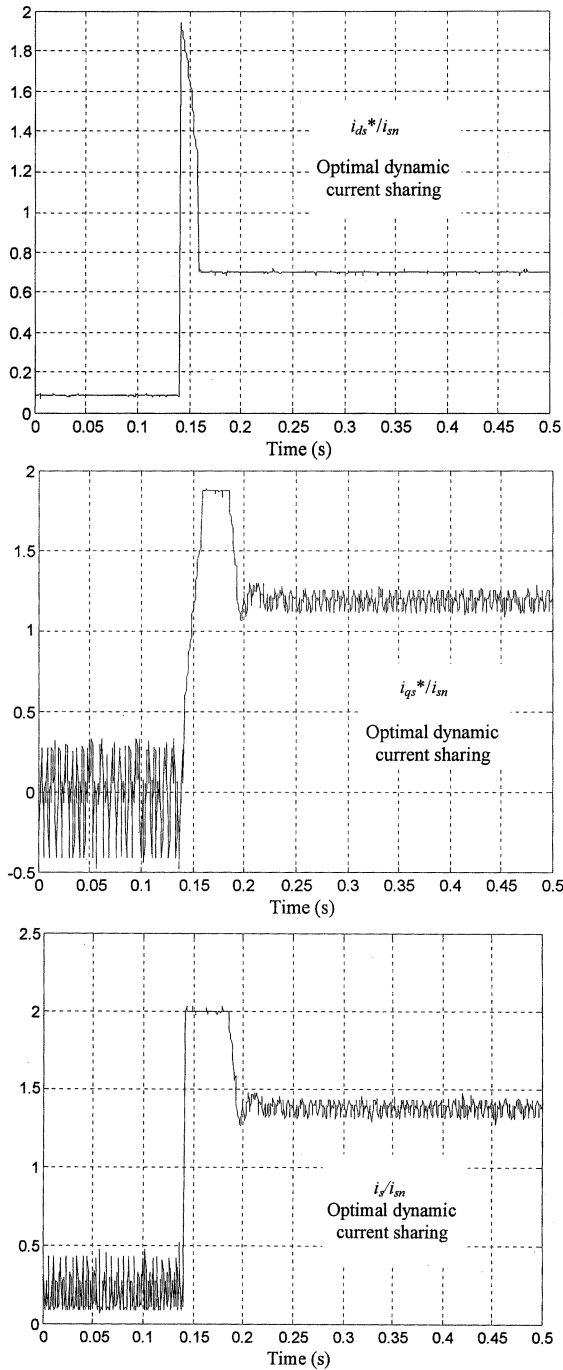


Fig. 4. Experimental results for the 2.2-kW motor after sudden load torque change from zero to 25 Nm: stator  $d$ -axis current command, stator  $q$ -axis current command, and total stator current in per unit for the proposed algorithm of optimal dynamic current sharing.

$d$ -axis current after a few milliseconds begins to decrease (in contrast to the method where full maximum stator current is at first assigned to the  $d$ -axis and then is switched to the  $q$ -axis). The net consequence of the difference in the  $d$ - $q$  axis current behavior with these two methods is a substantial difference in the maximum speed drop, illustrated in Fig. 6. When the stator  $d$ -axis current is reset to the rated value, the speed drops by around 36 rad/s and the time interval required to return the speed to the commanded value is almost 100 ms. In contrast to this, optimal dynamic current sharing enables the speed to recover

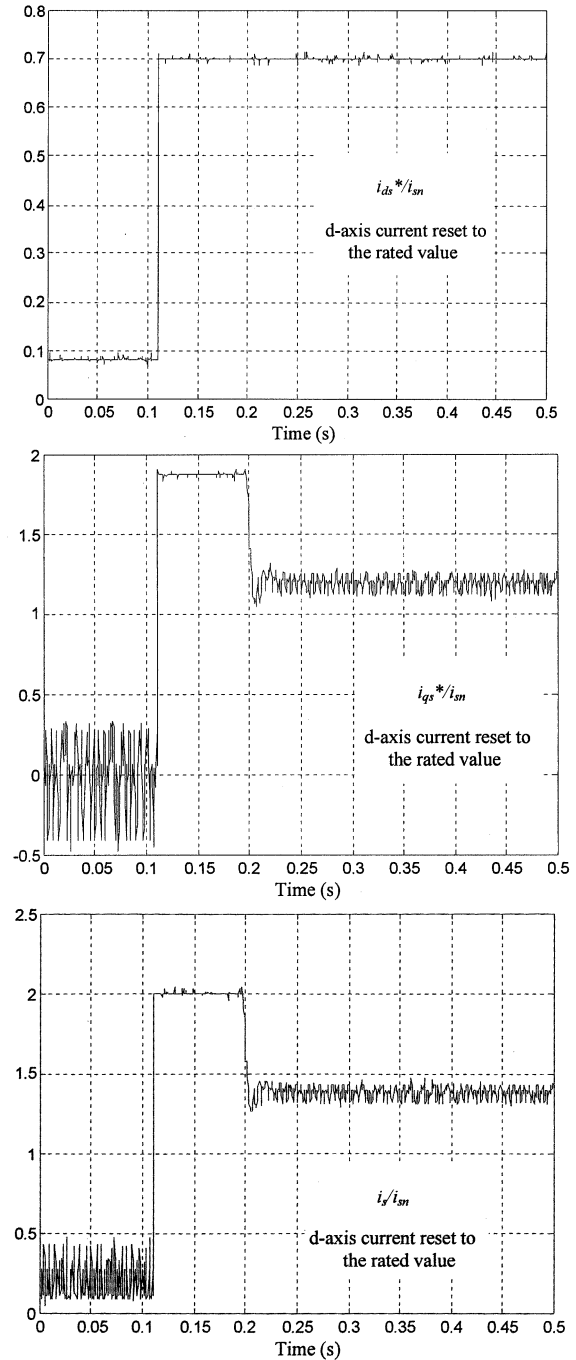


Fig. 5. Experimental results for the 2.2-kW motor after sudden load torque change from zero to 25 Nm: stator  $d$ -axis current command, stator  $q$ -axis current command, and total stator current in per unit when the stator  $d$ -axis current is reset to the rated value.

in less than 60 ms, since the maximum speed drop is only 25 rad/s. As can be seen from Figs. 4 and 6, stator  $d$ -axis current in the optimal dynamic current sharing strategy is reset to the rated value once when the minimum speed has been attained, as explained in Section II-C.

The next experiment illustrates the case when there is a mismatch between the load torque value assumed in calculations and the actual load torque value that occurs during the drive operation. The load torque is in (20) retained as equal to 25 Nm, while the actual step load torque applied to the machine is only

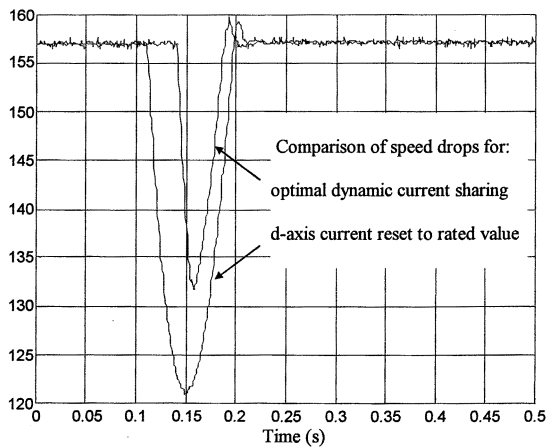


Fig. 6. Comparison of the experimentally recorded speed drops for the 2.2-kW induction motor drive (load torque stepped to 25 Nm) using proposed algorithm of optimal dynamic current sharing and the resetting of the stator *d*-axis current to the rated value.

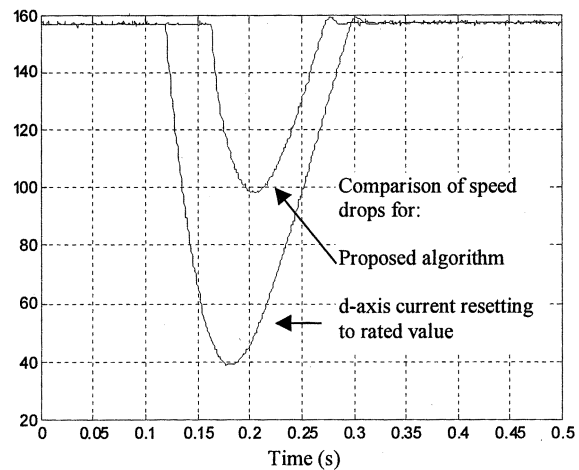


Fig. 8. Comparison of the experimentally recorded speed drops for the 2.2-kW induction motor drive (load torque stepped to 50 Nm) using proposed algorithm of optimal dynamic current sharing and the resetting of the stator *d*-axis current to the rated value. Inverter current limit is now increased to three times the rated stator current.

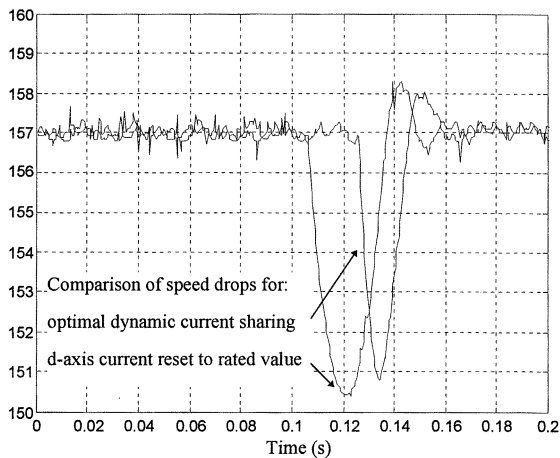


Fig. 7. Comparison of the experimentally recorded speed drops for the 2.2-kW induction motor drive (load torque stepped to 15 Nm with 25 Nm still used in calculations) using proposed algorithm of optimal dynamic current sharing and the resetting of the stator *d*-axis current to the rated value.

the rated torque value of 15 Nm. Since all of the current traces are similar to those shown in Figs. 4 and 5, only a comparison of the speed traces for the two methods of maximum current distribution is depicted in Fig. 7. The speed drop with both methods is now significantly smaller (less than 7 rad/s) and is comparable. The improvement in the speed drop value, provided by the proposed algorithm of optimum dynamic current sharing, is substantially smaller than in the previous case (only around 0.5 rad/s), due to the relatively small load torque value and the mismatch between the load torque value used in calculations (25 Nm) and the actual load torque impact (15 Nm). Optimal dynamic current sharing does still provide slightly smaller speed drop, when compared with the method of *d*-axis current resetting to the rated value. Even more important, however, is the improvement in the speed recovery time, provided by the optimal dynamic current strategy. As can be seen from Fig. 7, although the speed drops are of a comparable value, the time it takes to the first reference speed crossing is approximately 30 ms with the *d*-axis current resetting to the rated value. This time interval is reduced to only 18 ms with the optimal dynamic current sharing

strategy. Fig. 7 thus clearly proves that the proposed algorithm of optimal current distribution is advantageous even when the exact value of the load torque is not known.

Relative improvement in the performance of the proposed algorithm, when compared to the method of stator *d*-axis current resetting to the rated value, depends on the imposed current limit of the inverter. In general, the higher the maximum allowed inverter current is, the greater the improvement will be. In order to prove this statement, an experiment, similar to the one depicted in Fig. 6, is performed, again with the 2.2-kW motor drive. The maximum allowed inverter current is however now increased from twice to three times the rated stator current. The drive initially operates under the same no-load conditions as for Fig. 6 and at the speed of 157 rad/s. A step load torque, equal to 50 Nm, is then applied (this value is used in online calculations). The speed drops that result with the proposed algorithm and with the method of stator *d*-axis current resetting to rated value are shown in Fig. 8. As can be seen in Fig. 8, the speed drop attains the value of almost 120 rad/s if stator *d*-axis current is reset to the rated value. The proposed algorithm gives the speed drop of just below 60 rad/s, indicating that the reduction in the speed drop achieved with the proposed algorithm is 60 rad/s. This is substantially more than in Fig. 6, where the reduction in the speed drop was 11 rad/s. The explanation for this improvement is that, with a higher inverter current limit, the proposed algorithm assigns initially more current into the *d*-axis (almost three times rated stator current in the case of Fig. 8), thus achieving a quicker forced rotor flux build-up.

In industrial drives, inverter current limit is usually at least two times rated stator current for transients (the drive used here is rated for 8 A continuous, 22 A short-term; hence, three times rated current is just over the allowed current limit and can be sustained only on a very short-term basis). The two situations shown in Figs. 6 and 8 therefore cover the practical range of current limits. If for any reason inverter current limit were to be very low, of the order of rated stator current only, the improvement in transient response obtainable with the proposed



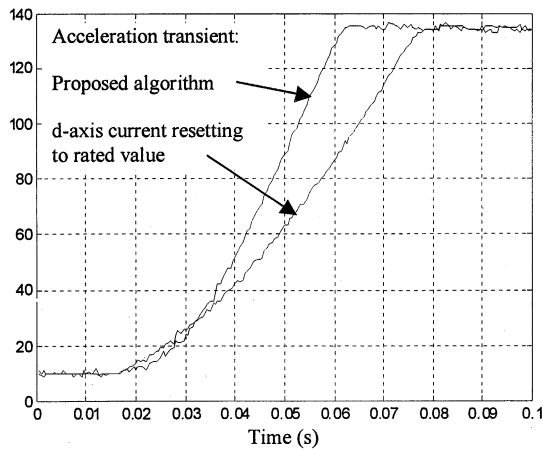


Fig. 9. Speed response for acceleration transient from 10 to 132 rad/s under no-load conditions with the proposed algorithm and with resetting of the stator  $d$ -axis current to the rated value ( $i_{s\max} = 2i_{sn}$ ).

algorithm over the stator  $d$ -axis current resetting to rated value would have been marginal.

The last experiment is related to the acceleration transient starting from low-speed, light-load operating condition. The 2.2-kW machine is initially operated under no-load conditions (approximately 1-Nm loading) at a speed of 10 rad/s. In order to achieve acceleration with the inverter current in the limit (which is again twice the rated stator current), a large speed command of 132 rad/s is applied. Note that this is below the rated speed of 157 rad/s. A lower value of the speed reference is selected in order to preserve full current control capability during the transient, by not entering the drive's voltage limit. Speed responses obtained with the proposed algorithm and with the method of stator  $d$ -axis current resetting are shown in Fig. 9. Resetting of stator  $d$ -axis current to the rated value initially provides a faster speed response, since substantial amount of current is immediately assigned to the  $q$ -axis. However, the speed response with optimum dynamic current sharing quickly catches up and then becomes considerably faster, yielding a substantial reduction in the overall duration of the transient.

#### IV. CONCLUSION

The paper proposes a novel dynamic algorithm for optimal maximum stator current distribution into the flux-producing and the torque producing current during a sudden load torque impact occurring at light load, low flux initial operating state. The method is developed by considering the magnetic circuit saturation and by accounting for the dynamic rotor flux change during such a transient. It is primarily aimed at optimum efficiency vector controlled induction motor drives.

Detailed derivation of the optimal current sharing algorithm is provided, together with a discussion of some important implementation related issues. It is shown that the problem reduces to the determination of the optimal current angle in each sampling instant and that the solution can be found by implementing on-line calculation of the square root function. A method for square root calculation in a DSP environment is described.

Verification of the proposed method is provided by both simulation and experimental investigation on two induction ma-

chines. The proposed optimal dynamic current sharing technique is compared with respect to the performance obtainable by the two known methods. It is shown that the algorithm provides a superior behavior, resulting in a smaller speed drop and a shorter speed recovery time, especially in the case when the value of the load torque impact is predictable from the known process in which the drive is used. The impact of the inverter current limit setting is examined and it is shown that, relative to the stator  $d$ -axis current resetting to the rated value, improvement in the response becomes more and more significant as the current limit is increased. Finally, superiority of the proposed algorithm with respect to the stator  $d$ -axis current resetting to the rated value is demonstrated for an acceleration transient with large step speed command change under light load condition.

#### REFERENCES

- [1] F. Abrahamsen, F. Blaabjerg, J. K. Pedersen, and P. B. Thogersen, "Efficiency optimized control of medium-size induction motor drives," in *Proc. IEEE Ind. Applicat. Soc. Annu. Meeting*, 2000, pp. 1489–1496.
- [2] F. Abrahamsen, J. K. Pedersen, and F. Blaabjerg, "State-of-art of optimal efficiency control of low cost induction motor drives," in *Proc. Power Electron. Motion Contr. Conf.*, vol. 2, 1996, pp. 163–170.
- [3] J. M. Moreno-Eguilaz and J. Peracaula, "Efficiency optimization for induction motor drives: past, present and future," in *Proc. Electrimacs*, 1999, pp. I.187–I.191.
- [4] G. S. Kim, I. J. Ha, and M. S. Ko, "Control of induction motors for both high dynamic performance and high power efficiency," *IEEE Trans. Ind. Electron.*, vol. 39, pp. 323–333, Aug. 1992.
- [5] D. S. Kirschen, D. W. Novotny, and T. A. Lipo, "Optimal efficiency control of an induction motor drive," *IEEE Trans. Energy Conversion*, vol. EC-2, pp. 70–76, Mar. 1987.
- [6] G. C. D. Sousa, B. K. Bose, and J. G. Cleland, "Fuzzy logic based on-line efficiency optimization control of an indirect vector-controlled induction motor drive," *IEEE Trans. Ind. Electron.*, vol. 42, pp. 192–198, Apr. 1995.
- [7] I. Kioskeridis and N. Margaris, "Loss minimization in scalar-controlled induction motor drives with search controllers," *IEEE Trans. Power Electron.*, vol. 11, pp. 213–220, Mar. 1996.
- [8] M. Ta-Cao and Y. Hori, "Convergence improvement of efficiency-optimization control of induction motor drives," in *Proc. IEEE Ind. Applicat. Soc. Annu. Meeting*, 2000, CD-ROM Paper no. 38\_04.
- [9] I. Kioskeridis and N. Margaris, "Loss minimization in induction motor adjustable-speed drives," *IEEE Trans. Ind. Electron.*, vol. 43, pp. 226–231, Feb. 1996.
- [10] I. T. Wallace, D. W. Novotny, R. D. Lorenz, and D. M. Divan, "Increasing the dynamic torque per ampere capability in saturated induction machines," *IEEE Trans. Ind. Applicat.*, vol. 30, pp. 146–153, Jan./Feb. 1994.
- [11] —, "Verification of enhanced dynamic torque per ampere capability in saturated induction machines," *IEEE Trans. Ind. Applicat.*, vol. 30, pp. 1193–1201, Sept./Oct. 1994.
- [12] Z. Cucej and D. Borojevic, "Input power minimization at inverter fed induction motor drive system with FOC by field weakening," in *Proc. IEEE Power Electron. Spec. Conf.*, 1997, pp. 1493–1499.
- [13] J. H. Chang and B. K. Kim, "Minimum-time minimum-loss speed control of induction motors under field-oriented control," *IEEE Trans. Ind. Electron.*, vol. 44, pp. 809–815, Dec. 1997.
- [14] D. S. Kirschen, D. W. Novotny, and T. A. Lipo, "On-line efficiency optimization of a variable frequency induction motor drive," *IEEE Trans. Ind. Applicat.*, vol. IA-21, pp. 610–616, July/Aug. 1985.
- [15] S. Sangwongwanich, M. Ishida, S. Okuma, and K. Iwata, "Manipulation of rotor flux for time-optimal single-step velocity response of field-oriented induction machines," *IEEE Trans. Ind. Applicat.*, vol. IA-24, pp. 262–270, Mar./Apr. 1988.
- [16] S. Yamanaka, H. Funato, L. Wang, and K. Kamiyama, "An improvement on a transient torque response in high efficiency control of induction motor drives," in *Proc. Power Electron. Motion Contr.*, 1998, pp. 5.241–5.246.
- [17] E. Levi, M. Sokola, and S. N. Vukosavic, "A method of magnetising curve identification in rotor flux oriented induction machines," *IEEE Trans. Energy Conversion*, vol. 15, pp. 157–162, June 2000.

- [18] E. Levi and V. Vuckovic, "Field-oriented control of induction machines in the presence of magnetic saturation," *Elec. Mach. Power Syst.*, vol. 16, no. 2, pp. 133–147, 1989.
- [19] E. Levi, S. Vukosavic, and V. Vuckovic, "Saturation compensation schemes for vector controlled induction motor drives," in *Proc. IEEE Power Electron. Specialists Conf.*, 1990, pp. 591–598.

**Slobodan N. Vukosavic** (M'93) was born in Sarajevo, Bosnia and Hercegovina, Yugoslavia, on January 27, 1962. He received the B.S., M.S., and Ph.D. degrees from the Electrical Engineering Faculty at the University of Belgrade, Belgrade, Yugoslavia, in 1985, 1987, and 1989, respectively.

Currently, he is the Project Leader with the Vickers Co., Milano, Italy, guiding the hardware and software R/D teams in designing high performance servo amplifiers and drives for industrial robots and general automation. He conducted the research in the areas of static power converters and microcomputer-based control of electrical drives at the Nikola Tesla Institute, Belgrade, Yugoslavia, until 1988, when he joined the ESCD Laboratory of Emerson Electric, St. Louis, MO, in the co-operative appliance drive research program. He is also an Associate Professor at the University of Belgrade, where he has been since 1995. His scientific interests are in the areas of the electromechanical conversion, modeling, and identification, digital signal processor (DSP)-based power conversion control, and power electronics. He has published many articles and several student textbooks, presented several invited papers, and completed many large scale R/D and industrial projects. He is also a reviewer for a number of scientific journals.

Dr. Vukosavic is a founding member of the ELTRAN Society and the board member of EE and Juzel societies.

**Emil Levi** (S'89–M'92–SM'99) was born in 1958 in Zrenjanin, Yugoslavia. He received the Diploma degree from the University of Novi Sad, Yugoslavia, and the M.Sc. and the Ph.D. degrees from the University of Belgrade, Belgrade, Yugoslavia, in 1982, 1986, and 1990, respectively.

Currently, he is Professor of electric machines and drives in the School of Engineering at Liverpool John Moores University, Liverpool, U.K. In 1982, he joined the Department of Electrical Engineering at the University of Novi Sad, where he became Assistant Professor in 1991. He joined Liverpool John Moores University in May 1992 as a Senior Lecturer. From 1995 to 2000, he was a Reader in Electrical Power Engineering. His main areas of research interest are modeling and simulation of electric machines, control of high performance drives, and power electronic converters. He has published over 130 papers, including more than 30 papers in major international journals.